Four wave mixing at air-dielectric interfaces with a femtosecond laser excitation

R. Sai Santosh Kumar, Suneel Singh, and D. Narayana Rao*

School of Physics, University of Hyderabad, Hyderabad 500 046, India
*dnrsp@uohyd.ernet.in

Abstract: In this article we report our experimental results on non collinear four-wave mixing (FWM) at air-dielectric interfaces. We generated FWM signal from the two interfaces of a 1mm thick fused silica slide with air using two 800 nm, 100 fs pump pulses in non-collinear pump-probe type geometry. We observe that there is a maximum peak shift of ~1.5 nm in FWM signals corresponding to the two interfaces of the same silica slide. Further, we find that the intensity of FWM signal observed at air to silica interface is less than that from silica to air interface. We briefly elaborate on this observation with systematic study of FWM in fused silica.

OCIS codes: (190.4380) Nonlinear optics, four-wave mixing; (190.4350) Nonlinear optics at surfaces; (190.2110) Ultrafast Nonlinear Optics; (320.2250) Femtosecond Phenomena.

References and links

1. Y. R. Shen, *The Principles of Nonlinear Optics,* (Wiley-Interscience, New York, 1984).
2. N. Bloembergen, R. K. Chang, S. S. Jha, and C. H. Lee "Optical second harmonic generation in reflection from media with inversion symmetry," Phys. Rev. **174**, 813-822 (1968).
3. C. K. Chen, A. R. B. de Castro, and Y. R. Shen, "Surface-Enhanced Second-Harmonic Generation", Phys. Rev. Lett. **46**, 145-148 (1981).
4. C. C. Wang and A. N. Duminiski, "Second harmonic generation of light at the boundary of alkyl halides and glasses," Phys. Rev. Lett. **20,** 668-671 (1968).
5. P. Guyot-Sionnest, W. Chen, and Y. R. Shen, "General considerations on optical second-harmonic generation from surfaces and interfaces," Phys. Rev. B **33**, 8254-8263 (1986).
6. Y. R. Shen, "Surface properties probed by second harmonic and sum frequency generation," Nature **337**, 519-525 (1989).
7. T. Y. F. Tsang, "Optical third-harmonic generation at interfaces," Phys. Rev. A. **52**, 4116 (1995).
8. R. L. Sutherland with contributions by D. G. McLean and S. Kirkpatrick, *Handbook of Nonlinear Optics*, Second Edition, Revised and Expanded (New York, NY: Marcel Dekker) (2003).
9. D. Meshulach, Y. Barad, and Y. Silberberg, "Measurement of ultrafast optical pulses by third-harmonic generation," J. Opt. Soc. Am. B **14**, 2122 – 2125 (1997).
10. Y. Barad, H. Eisenberg, M. Harowitz, and Y. Silberberg, "Nonlinear scanning laser microscopy by third harmonic generation," Appl. Phys. Lett. **70**, 922-924 (1997).
11. G. Veres, S. Matsumoto, Y. Nabekawa, and K. Midorikawa, "Enhancement of third-harmonic generation in absorbing media," Appl. Phys. Lett. **81**, 3714-3716 (2002).
12. V. Shcheslavskiy, G. Petrov, and V. V. Yakovlev, "Nonlinear optical susceptibility measurements of solutions using third-harmonic generation on the interface," Appl. Phys. Lett. **82**, 3982 (2003).
13. R. S. S. Kumar, S. S. Harsha, and D. N. Rao, "Broadband supercontinuum generation in a single potassium di-hydrogen phosphate (KDP) crystal achieved in tandem with sum frequency generation," Appl. Phys. B **86**, 615 - 621 (2007).
14. M. Samoc, A. Samoc, B. L. Davis, "Third harmonic autocorrelation and wave-mixing in a thin film of poly(p-phenylenevinylene)," Opt. Express **11**, 1787 -1792 (2003), http://www.opticsexpress.org/abstract.cfm?uri=OE-11-15-1787.
15. Th. Schneider, R. P. Schmid, and J. Reif, "Efficient self phase matched third harmonic generation of ultrashort pulses in a material with positive dispersion," Appl. Phys. B. **72**, 563 - 565 (2001).

1. Introduction

It is generally accepted that the breaking of inversion symmetry at any interface between two media with inversion symmetry causes structural asymmetry and local field variation across

#98470 - $15.00 USD Received 8 Jul 2008; revised 29 Aug 2008; accepted 8 Oct 2008; published 21 Oct 2008

the surface layer. This gives rise to discontinuity in the normal component of the electric field and an induced nonlinear polarization containing high-order nonlinear susceptibility tensors. Good literature is available on the second harmonic generation (SHG) at the surfaces of different materials [1]. It was found that in a medium with inversion symmetry, the surface contribution to SHG could be comparable with or dominant over the bulk contribution [1-5]. Numerous applications were based on surface enhancement of second order susceptibility $\chi^{(2)}$ of a medium as a powerful and effective diagnostic tool [6]. On the other hand, though third order nonlinear optical process is allowed in all materials independent of the symmetry property of the medium, the surface third order susceptibilities $\chi^{(3)}$ were given lesser consideration because generally it is much weaker and thus requires high intensities. Nevertheless, with recent advances in ultrafast laser technology that enable attainment of high peak powers with relatively inexpensive and low-average power lasers, this particular drawback could easily be overcome. Tsang [7] experimentally demonstrated using femtosecond laser pulses that the normally weak but electric dipole allowed THG process can be appreciably strong at an air-dielectric interface and thus may contain useful surface characteristics. Efficiency of the THG at interfaces near the focal point of a tightly focused laser beam has led to numerous applications such as in ultrashort pulse characterizations, microscopy and third order nonlinear characterization of both absorbing and non-absorbing media [8-12]. Four-wave mixing (FWM), which is also a consequence of $\chi^{(3)}$ of the materials, plays a very important role in many applications [8]. Numerous reports in literature deal with the FWM both in degenerate and non-degenerate geometry and usually are generated within the bulk of the sample. In this article, we have investigated four wave mixing (FWM) at silica-air interfaces using a femtosecond (fs) laser. A systematic study of FWM is reported for the two interfaces of a 1mm fused silica slide. We made the following observations in the course of our study: (i) there is a maximum peak shift of 1.5 nm in the FWM spectra from air-glass interface; (ii) intensity of the FWM signal at air to silica interface is weaker compared to FWM signal at silica to air interface.

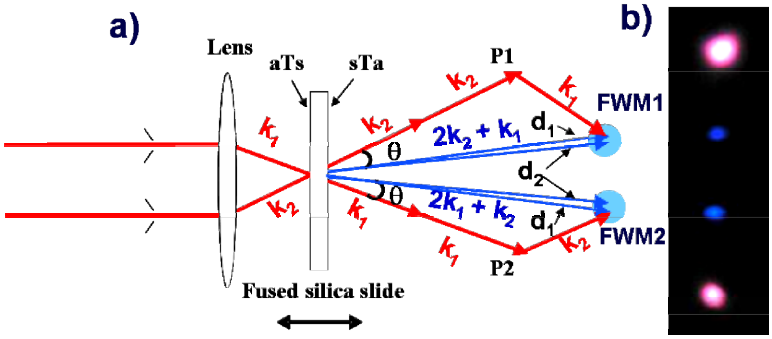

Fig. 1. (a) Experimental set-up used in the study; (b) Snap-shot of the FWM observed as blue fluorescence on a paper screen.

2. Experiment

In the present study we use two pumps in a simple non-collinear pump-probe type of arrangement as shown in Fig. 1. The details of the laser system used can be found in an earlier report [13]. The fundamental IR pulses from an amplified Ti: Sapphire laser (Maitai + Spitfire, Spectra Physics) used in the study are centered at 800 nm having a pulse width of 100 fs and a bandwidth of 13 nm. The pulse width was determined from the second order intensity auto-correlation using a nonlinear crystal. The two fundamental beams of

#98470 - $15.00 USD Received 8 Jul 2008; revised 29 Aug 2008; accepted 8 Oct 2008; published 21 Oct 2008

approximately equal average power and beam size of 2 mm are focused onto the 1 mm fused silica slide by a focusing lens of focal length of 100 mm making an angle of 10^0 on the sample with respect to each other. The Rayleigh range and the beam waist of each beam are calculated to be ~2 cm and ~50 μm respectively, in the Gaussian approximation. The interaction length L, of region of overlap of the two beams is ~300 μm. The choice of the focal length of the lens is such that (i) there is optimal peak intensity for the generation of FWM signal in the focal volume, (ii) the interaction region of the two beams is such that the two interfaces of the silica slide can be distinguished and (iii) that no continuum is generated. The nomenclature of the two interfaces, followed throughout the report is as shown in Fig. 1(a): aTs refers to the air to silica interface and sTa refers to the second interface i.e., silica to air with respect to the propagation of the fundamental beam. The silica slide is mounted on a translational stage and moved across the focal position of the converging beams in steps of 30 μm from one interface position to the other through the center of the slide. The FWM spectra is recorded at each position and analyzed by coupling the beams directly into the spectrometer positioned close to the slide. When the two fs pulses overlap temporally and spatially we see the FWM as two blue spots in between the IR spots as shown Fig. 1(b). The FWM is detected by coupling the output into spectrometer (Ocean Optics Inc., model SD2000 with spectral range of 200–1000 nm) interfaced to a personal computer. All the data presented in this study are taken with respect to FWM1 beam and is observed to be the same with FWM2.

3. Results and discussion

We observe the FWM at input intensities of fundamental pulses (P1 and P2) in the range of 400 – 800 GW/cm^2 well below the intensities required for the continuum generation (~1000 GW/cm^2) in the fused silica. Figure 2(a) shows the FWM spectra recorded at the two interfaces. Clearly the FWM at aTs has a peak at 267.3 nm and the FWM signal due to sTa appear at 268.8 nm, a peak shift of ~1.5 nm. The observed full width at half maximum ($\Delta\lambda$) of the FWM signal at sTa ($\Delta\lambda$ = 3.8 nm) is found to be broader than the FWM signal at aTs ($\Delta\lambda$ = 2.4 nm). As seen in the Fig. 1, the FWM signals FWM1 and FWM2 are generated with an angular separation of 3.4^o – 3.6^o with P1 and P2 respectively. The earlier reports [14, 15] with similar experimental configuration do not discuss the surface effects and refer to this observed signal as THG without recording the spectral content. This paper refers to this signal as FWM signal since it represents the interaction between different wave vectors and frequencies. We did not observe any FWM signal in the bulk, i.e., at the center of the silica slide for the power level used in the study, while we observe FWM only at the two interfaces. In order to verify that the peak-shift is not an artifact we sent a He-Ne laser beam as a reference collinear with one of the 800 nm beams and the scattered beam is recorded along with the FWM signal. He-Ne laser beam does not show any shift in its spectrum. In order to avoid the effects of dispersion of fiber, the FWM signal is directly coupled into the slit of the spectrometer rather than coupling it through a fiber.

As we translate the fused silica slide across the focal point we observe the following: (i) the FWM signal increases as the aTs approaches the focus and then decreases as it moves away from the focus; (ii) no observable signal in the bulk and (iii) the signal increases gradually till sTa and then decreases as the focal positions moves out of the silica slide. Figure 2(b) shows the signal strength as a function of the position of the silica slide considering the center of the slide as the reference point. Clearly, we see that owing to the interaction length of the two beams, the FWM signal is seen for 300 μm about the two interfaces and no signal for 300 μm about the center. The error bars shown in the Fig. 2(b) are representatives of the experimental error of 20%, which is reasonable considering the weak signals involved. This error is estimated by repeating the experiment as many as three times. From the Fig. 2 we draw an important conclusion that the intensity of the FWM from aTs is much weaker

#98470 - $15.00 USD Received 8 Jul 2008; revised 29 Aug 2008; accepted 8 Oct 2008; published 21 Oct 2008

compared to FWM from sTa and that both these signals are several orders larger than the bulk value.

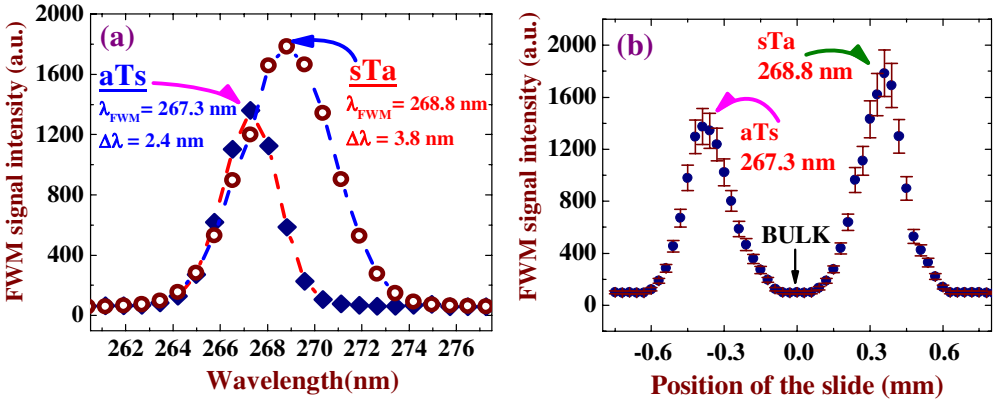

Fig. 2. (a) FWM peaks as observed at the two interfaces aTs and sTa. The dashed line is just to guide the eye the scatter of the obtained experimental FWM data showing the symmetry of the FWM signal; (b) the variation of the FWM intensity as the fused silica slide is moved across the focal spot of the lens.

This observation agrees well with the earlier reports, where the third-order nonlinear susceptibility of bulk amorphous fused silica $\chi^{(3)}_{bulk}$ (~ 1.4 x 10^{-14} esu) [8] is found to be much lower than that at the surface $\chi^{(3)}_{surface}$ (~10^{-11} esu) [7]. The FWM signal as usual is found to increase cubically with increase in the input beam intensity confirming the third order nonlinear process. Figure 3(a) is a 3D plot of the intensity of the FWM signal against the slide position. Clearly we find that no signal is generated at the center of the slide. Figure 3(b) is a grey scale image plot of the FWM spectra showing the spectra plotted as a function of slide position.

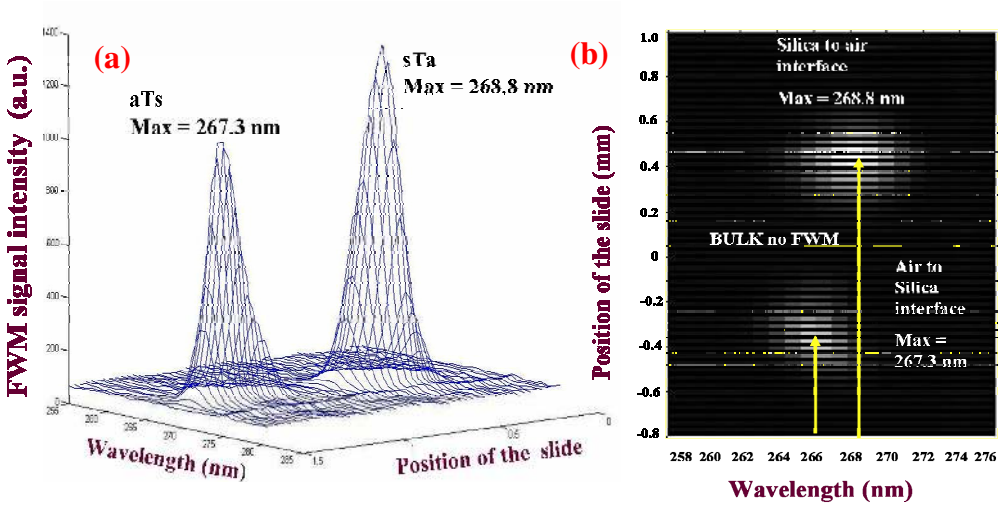

Fig. 3. (a) A 3-D plot showing the FWM spectra at various positions in the silica slide; (b) The spectra plotted as a 2D plot of spectra vs position of the slide.

#98470 - $15.00 USD Received 8 Jul 2008; revised 29 Aug 2008; accepted 8 Oct 2008; published 21 Oct 2008

We can explain the observed peak-shift of FWM through the following phase matching considerations. As the Rayleigh range is 2 cm, we can consider the two interacting beams over the interaction region of 300 μm as plane waves. The FWM geometry is shown in Fig. 1(a), where the pump beams are represented by the wave vectors $\mathbf{k_1}$ and $\mathbf{k_2}$. The generated phase matched FWM signals at $2\mathbf{k_1}+\mathbf{k_2}$ and $\mathbf{k_1}+2\mathbf{k_2}$ respectively, appear well separated from the fundamentals $\mathbf{k_1}$ and $\mathbf{k_2}$ at an angle θ. Considering the input fundamentals $\mathbf{k_1}$ and $\mathbf{k_2}$ to be centered at 800 nm [Fig. 4(a) dotted curve] the calculated $\mathbf{k_1}+2\mathbf{k_2}$ has a magnitude of 267.5 nm and a calculated value of θ to be 3.3^0. Thus we find that the calculated FWM signal and θ values are in very good agreement with the measured FWM signal of 267.3 nm from aTs interface. Similarly we recorded the spectrum of the fundamental just when the focus is at sTa interface. The spectra are shown as solid curve in Fig. 4(a). Clearly the spectral profile of fundamental is changed drastically as the pulse travels through the silica slide with the peak being split into two dominant peaks centered at 799 nm and 806 nm and a small peak centered at 788 nm. In order to explain the observed FWM signal the spectrometer slit (25 μm) is scanned across the FWM signal spots. For the direction which is away from the center of the pattern (direction d_1 in Fig. 1(a)) the spectral peak appears at 268.8 nm and when the slit is moved towards the center of the pattern (direction d_2 in Fig.1) the peak appears at 268.0 nm indicating wave mixing of different **k-**wave vectors of the dispersed fundamental beam at the second surface. Following discussion pertains to only one position of the slit (d_1) where 806 nm ($\mathbf{k_1}$) mixes with 799 nm ($\mathbf{k_2}$). The data is found to match exactly for the mixing of 799 nm ($\mathbf{k_1}$) and 806 nm ($\mathbf{k_2}$) leading to 268.0 nm. Figure 4(b) shows the theoretically simulated curve (solid line) for the FWM signal at $\mathbf{k_1}+2\mathbf{k_2}$ by deconvoluting the dispersed IR fundamental into two lines at 806 nm ($\mathbf{k_1}$) and 799 nm ($\mathbf{k_2}$). In order to arrive at the intensities observed at aTs and sTa surfaces, we have assumed different efficiencies for the FWM signals for mixing of 800 nm ($\mathbf{k_1}$) and 800 nm ($\mathbf{k_2}$) leading to 267.3 nm and the FWM signal at 268.8 nm for the fundamental beams recorded when the spectrometer slit is in position d_1 at 806 nm ($\mathbf{k_1}$) and 799 nm ($\mathbf{k_2}$). Dispersion in the silica slide gives rise to a distribution of spectrum along with corresponding wave vectors. Thus availability of a wide range of wave vectors due to dispersed spectrum at the second surface is assumed to lead to wave mixing with higher efficiency at the sTa surface. The values of Δλ for the simulated curves are also in close agreement with the observed FWM signals.

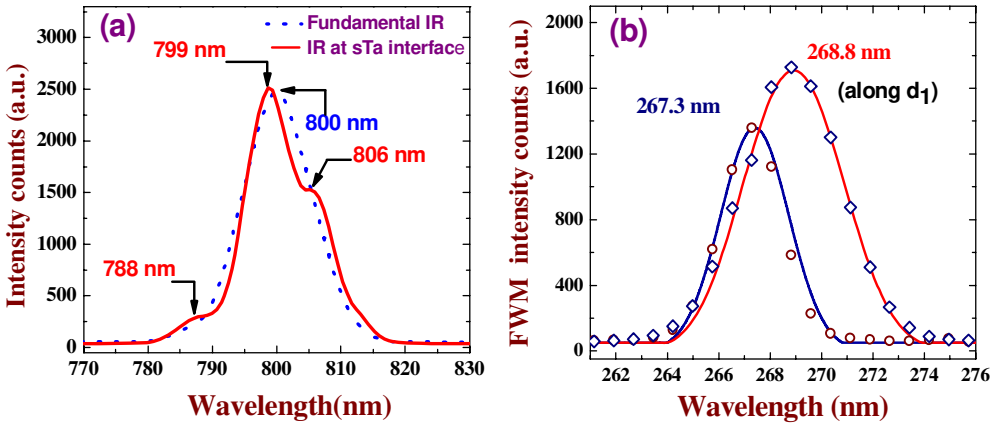

Fig. 4. (a) The dotted curve showing spectral profile of IR fundamental used for the study before focusing into the slide and solid line is the modified spectral profile of the fundamental while the focus is at sTa interface of the slide; (b) open circles and diamonds are the experimental data whereas the solid lines show the simulated curves for wave-mixing at aTs and sTa interfaces respectively taking into account the wave-mixing of all the spectral components present in the fundamental when the spectrometer slit at d_1.

#98470 - $15.00 USD Received 8 Jul 2008; revised 29 Aug 2008; accepted 8 Oct 2008; published 21 Oct 2008

The coherence length calculated for THG to occur in fused silica from the relation $l_c = \lambda_0/[6(n_{3\omega} - n_{\omega})]$ is ~ 3μm, where λ_0 is the wavelength of fundamental at 800 nm and $n_{3\omega}$ (= 1.499) and n_{ω} (= 1.453) are the refractive indices of fused silica at 267 nm and 800 nm respectively. As $\chi^{(3)}_{surface}$ is three orders of magnitude larger than $\chi^{(3)}_{bulk}$ and $L >> l_c$, translation of the slide across the interaction region results in the generation of FWM signal mainly due to significant contribution of $\chi^{(3)}_{surface}$ throughout the interaction region L. When the interaction region is entirely inside the bulk we observe no signal due to the effective cancellation of the generated signals as $L >> l_c$ and weak signals from the bulk. We generated the FWM signals using different focal length lenses (6 to 17cm) to alter the interaction length in the bulk and get odd multiples of the l_c for the interaction region. We still did not observe any signal in the bulk. If there is no enhancement in the nonlinearity at the surface, we should have observed signals while changing the interaction length in the bulk. We therefore conclude that the signals observed at the surfaces are due to the enhanced surface nonlinearities arising from the structural discontinuity and local fields caused by the field discontinuity at the interface. Also we did not see any THG in the direction of fundamental beam after passing through the glass slide indicating that the observed signals are purely due to FWM and are not due to THG. A summary of the experimentally observed and theoretically calculated values of various quantities is presented in Table 1, which are in good agreement. The observed differences are mainly due to the resolution of the spectrometer.

Table 1. Summary of the theoretical predictions for explaining the observed peak shift of FWM signal at the aTs and sTa.

	$\underline{\mathbf{k}}_{FWM} = \mathbf{k_1} + \mathbf{2k_2}$				θ		Δλ	
	$\lambda(\mathbf{k_1})$ (nm)	$\lambda(\mathbf{k_2})$ (nm)	λ_{FWM} (nm) Theory	λ_{FWM} (nm) Observed	Theory	Observed	Theory (nm)	Observed (nm)
aTs	800	800	267.5	267.3	3.3^0	3.5^0	2.6	2.4
sTa slit at d1	806	799	268.9	268.8	3.4^0	3.4^0	3.9	3.8
sTa slit at d2	799	806	268.2	268.0	3.5^0	3.6^0	3.0	3.7

4. Conclusions

In conclusion, we present here our observations of the surface enhanced FWM for the air - fused silica interfaces using a two beam non-collinear geometry by recording the FWM spectra at the two interfaces and the center of the slide. We find that there is enhanced FWM at the two interfaces with the FWM at sTa more intense than aTs and no FWM at the center of the slide. More interestingly we observe that there is maximum peak shift of ~1.5 nm in the FWM generated at the two interfaces.

Acknowledgments

Financial support from Department of Science and Technology (DST) is acknowledged. R.S.S. Kumar acknowledges the financial support of Council of Scientific and Industrial Research (CSIR).

#98470 - $15.00 USD Received 8 Jul 2008; revised 29 Aug 2008; accepted 8 Oct 2008; published 21 Oct 2008